Progress In Electromagnetics Research C, Vol. 134, 79–91, 2023

New Elliptical Miniaturized Antenna Using Concentric Open Rings for UWB Applications

Djamel Sayad[1, *], Chemseddine Zebiri[2], Huthaifa Obeidat[3], Issa Elfergani[4, 5], Alaedine Amroun[2], Merih Palandoken[6], Mohamed L. Bouknia[2], Rami Zegadi[2], and Jonathan Rodriguez[4]

Abstract—In this paper, a low-profile miniaturized microstrip monopole antenna with an overall size of 15 mm×20 mm×1.6 mm is developed and analyzed for Ultra-Wide Band (UWB) services. The proposed antenna is carefully designed, optimized, and analyzed using HFSS 15 simulation software. A prototype of the design is realized and experimentally tested as proof of concept. The results are discussed and compared with literature. They show attractive radiating features for UWB applications. The proposed antenna consists of an elliptical patch printed on a low-cost FR-4 epoxy substrate with a modified ground plane. To achieve UWB characteristics, elliptical rings are etched on the conducting patch, and the ground plane is modified by adding an inverted L shaped strip and creating a semi-elliptical slot in the partial ground opposite to the feed line. The achieved ultra-wide band ranges from 3.1 to 18.1 GHz (141.51%).

1. INTRODUCTION

Antenna technology has recently contributed to making huge leaps in the field of wireless communications. Microstrip antennas have been one of the most important pillars of antenna technology due to their attractive features, such as being low profile, conformable to planar and nonplanar surfaces, simple, inexpensive, easy to fabricate, mechanically robust, compatible with MMIC designs, and very versatile in terms of resonant frequency, polarization, and pattern. However, microstrip antennas have some operational drawbacks such as low radiation efficiencies and quite narrow bandwidths [1–3], which limits their use in UWB applications.

In some applications, such as in government security systems [1], digital still cameras, industrial colorimetric measurements, and spectral biological imaging, the use of narrow bandwidths is desirable [4, 5]. However, narrowband antennas are unable to handle quick pulses of nanosecond duration throughout the wider band of frequencies leading to dispersion and distorted signals [3]. Because UWB technology makes use of a broad range of frequencies typically between 3.1 and 10.6 GHz and their ability to support higher data transmission and multi-channel connectivity [2, 3, 6], it has been increasingly popular over the past few years.

UWB has expanded the operational frequency band to a broader range of applications by using signals of nanosecond or picosecond pulses. It provides an extremely wideband spectrum for existing radio technologies such as Wi-Fi, WLAN, WiMAX, and other cellular wide area communications

Received 3 April 2023, Accepted 22 May 2023, Scheduled 1 July 2023

* Corresponding author: Djamel Sayad (d.sayad@univ-skikda.dz).

[1] Laboratoire d'Electrotechnique de Skikda (LES), University 20 Aout 1955-Skikda, Skikda 21000, Algeria. [2] Laboratoire d'Electronique de puissance et commande industrielle (LEPCI), Department of Electronics, University of Ferhat Abbas, Sétif -1-, Sétif 19000, Algeria. [3] Department of Communications and Electronics Engineering, Faculty of Engineering, Jerash University, Jerash, Jordan. [4] The Instituto de Telecomunicações, Campus Universitário de Santiago, Aveiro 3810-193, Portugal. [5] School of Engineering and Informatics, University of Bradford, Bradford BD7 1DP, UK. [6] Department of Electrical and Electronics Engineering, Izmir Katip Celebi University, Izmir, Turkey.

replacing short-wired links [7–9]. Moreover, Internet of Things [10], health care [11], remote sensing [12], wearable applications [13], and microwave imaging [14] have all made use of UWB technology.

Recently, radar systems, detection of unexploded mines, health check of civil engineering structures and positioning location are other UWB applications that have also received significant attention [3, 15, 16].

The most influential challenges in UWB antenna design, particularly, are: realizing wideband with a satisfactory radiation efficiency and achieving a compact size at the lower operational frequency band. In this context, to achieve these specifications, a variety of designs of different shapes have been proposed in the literature. These include circular discs [17–19], rings [20–22], elliptical forms [23–25], and fractal patches [26–28]. Various techniques have been exploited to enhance the bandwidth such as the defected ground structure (DGS) [18, 23, 29–32], use of parasitic elements [29, 33, 34], introducing slits in the patch [34–39], loading stubs and shorting pins [40–42], and use of metamaterials that exhibit many special properties [7, 43, 44]. On the other hand, the UWB-based devices, when exploiting the full potential of the wide frequency band benefits, should not emit excessive energy to interfere with other narrower band systems nearby, while maintaining miniaturized sizes of antennas, which has become a very crucial requirement in the development of modern communication systems. This makes the design of UWB antennas a difficult challenge, since it must be capable of providing an extremely wide frequency band and still obey the Federal Communications Commission (FCC) standards.

Many small size UWB antenna designs with different structures operating in the 3.1 and 10.6 GHz range have been introduced; however, there is still a lot to be done regarding the design miniaturization and impedance bandwidth enhancement. The present work aims to further contribute to this subject and brings it forward. In this optic, a new UWB antenna design with more attractive compact size and radiation features, compared to recent works, is proposed.

For the last decade, researchers have approached the subject area in a number of different ways. Many studies have adopted circular or elliptical patches in antenna designs, due to their advantages to give suitable UWB features over the operating frequency range [20, 23–25, 45, 46]. Several previous studies have illustrated the advantage of using concentric slots for size reduction of the radiating structure and split ring resonators techniques to enhance the antenna impedance bandwidth [19, 47].

The design presented in this paper combines selected conventional techniques to meet the requirements of a practical UWB system, along with the use of elliptical concentric open rings (CORs). These latter are adopted as an alternative to split ring resonators (SRRs) that suffer from narrow bandwidth operation [48, 49]. The procedure introduces elliptical CORs on the patch resulting in a multitude of current paths. This helps to enhance the slow wave effect which effectively increases the length of the current path and the effective electrical length of the patch. Consequently, new resonating modes are created at lower frequencies which helps to reduce the design size.

2. ANTENNA CONFIGURATION

The design is based on an elliptical-patch monopole planar structure. To achieve UWB and miniaturization features, some alterations are brought to the basic structure. The ground plane is defected, and the patch is tilted 45°. The patch is modified by cutting elliptical thin slots resulting in six open concentric elliptical ring-shaped strips. Miniature dimensions are achieved with further improvement and other radiation characteristics. The designed antenna is printed on an FR-4 substrate having a compact size of $W \times L = 15 \times 20\,\text{mm}^2$, with a dielectric constant $\varepsilon_r = 4.4$, $\tan\delta = 0.02$, and thickness $h = 1.6\,\text{mm}$ (Fig. 1). The antenna is optimized using Ansys HFSS 15 and experimentally realized to validate the simulation results.

Initially, as shown in Fig. 1, the antenna consists of an elliptical copper patch of thickness $t = 0.035\,\text{mm}$ tilted 45° clockwise, with six elliptical open rings with equal openings (splits) of $W_{1-6} = 1.2\,\text{mm}$. Their positions (ϕ_{1-6}) are carefully optimized, and optimal values are adopted. Every two successive rings of width t_i are separated by a certain distance S_i.

The antenna is fed by a microstrip line crossed by a perpendicular strip as a matching stub to help achieve the required results. The modified ground plane consists of an inverted L strip with a semi-elliptical slot. All geometrical parameter dimensions are presented in Table 1.

A step by step design process of the proposed UWB antenna is described from the beginning to

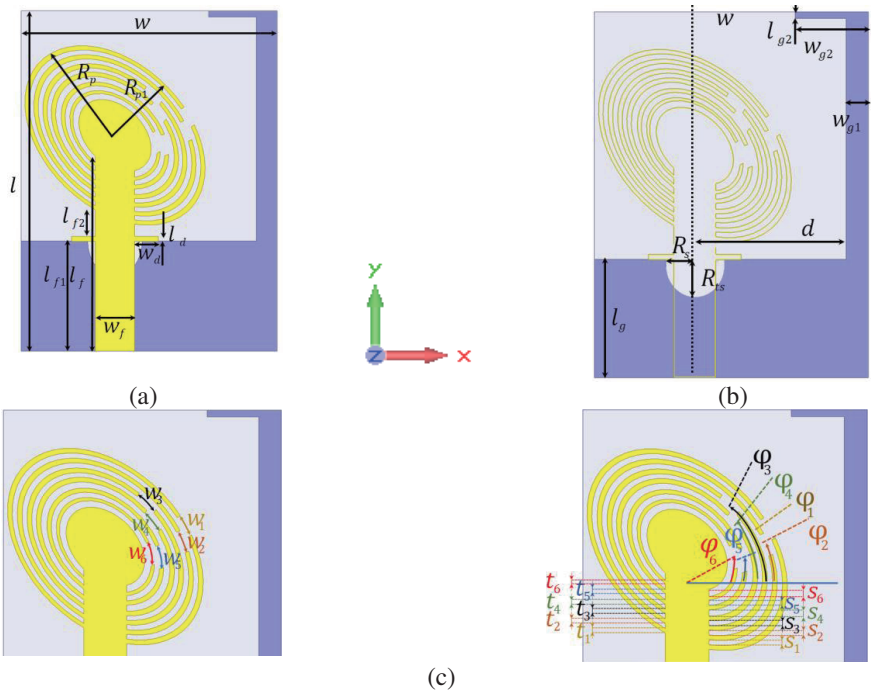

Figure 1. Proposed UWB antenna, (a) top view (b) bottom view and (c) detailed geometrical parameters.

Table 1. Geometrical parameters of the proposed antenna.

Parameter	Value (mm)	Parameter	Value (mm)	Parameter	Value (mm)
W	15	Ld	0.3	$t3$	0.24
L	20	Wd	1.38	$t4$	0.24
Lg	6.5	Rp	5.46	$t5$	0.22
$Wg1$	3.05	$Rp1$	4.2	$t6$	0.18
$Lg2$	0.3	$S1$	0.38	h	1.6
$Wg2$	4	$S2$	0.28	t	0.035
Rs	3.2	$S3$	0.33	φ_1	33°
Rts	2	$S4$	0.24	φ_2	25°
Wf	2.31	$S5$	0.26	φ_3	61°
Lf	11	$S6$	0.26	φ_4	50°
$Lf1$	6.475	$t1$	0.24	φ_5	21°
$Lf2$	1.5	$t2$	0.24	φ_6	28°

the final model along with an evaluation of the antenna parameters (S_{11} and gain) of each step until the desired results are reached.

As shown in Fig. 2, we start with a tilted elliptical patch and a regular rectangular ground plane (Ant.1), and some modifications and adjustments are brought to the structure, namely, cutting an elliptical slot (Ant.2) and adding an inverted L strip in the partial ground plane.

The S_{11} parameter of these first three structures is presented by Fig. 3. The rings are introduced to the radiating patch one by one (Fig. 4).

Improvements can be noticed in the antenna bandwidth due to the rings insertion (Fig. 5). After introducing 6 rings a lower frequency of 3.3 GHz is reached as a better result. This antenna shows a

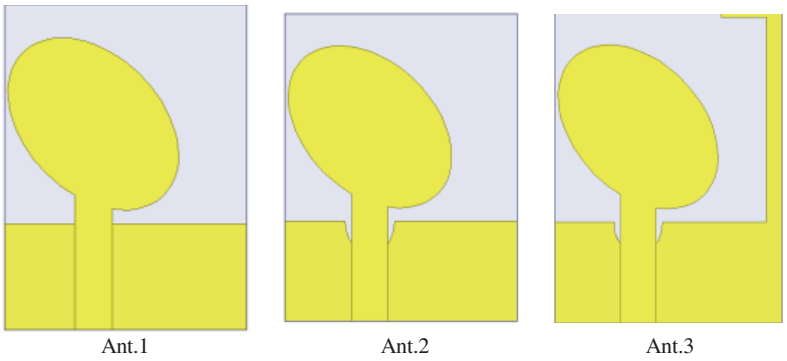

Figure 2. Modification steps of the ground plane.

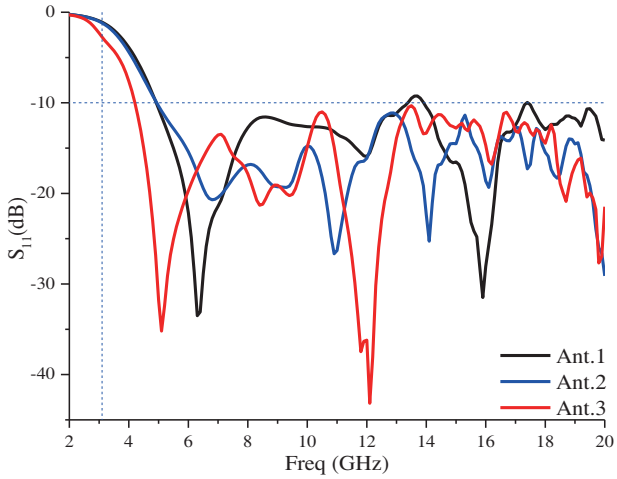

Figure 3. Effects of the ground plane on the S_{11} coefficient.

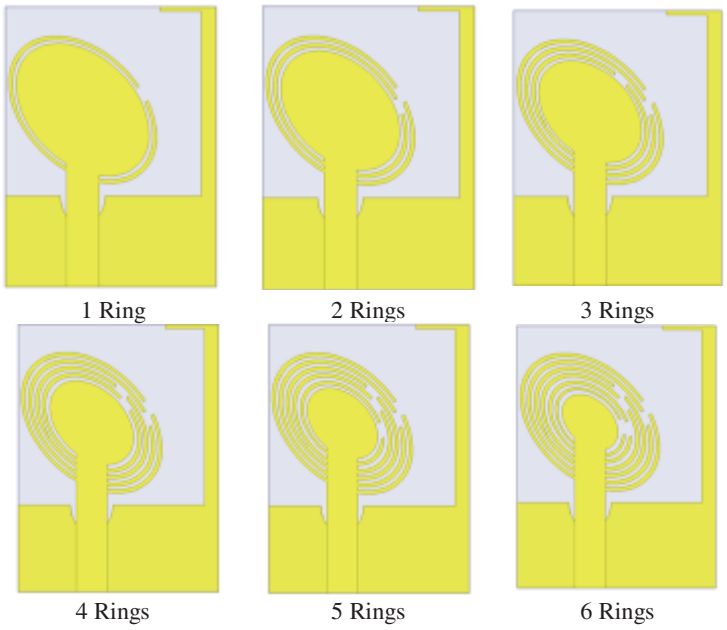

Figure 4. Rings introduction.

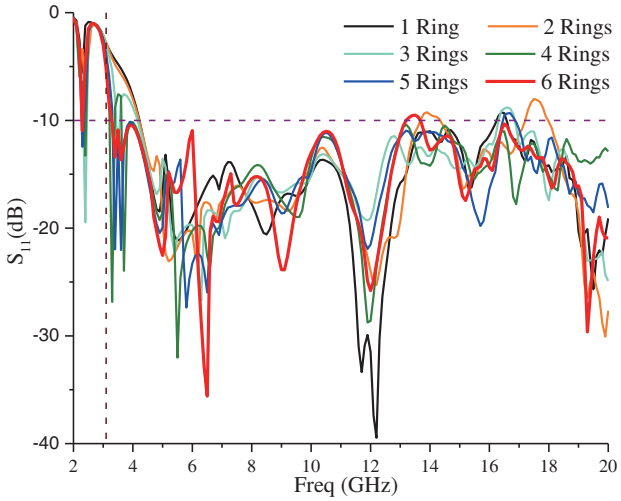

Figure 5. Effect of the rings on the S_{11} coefficient.

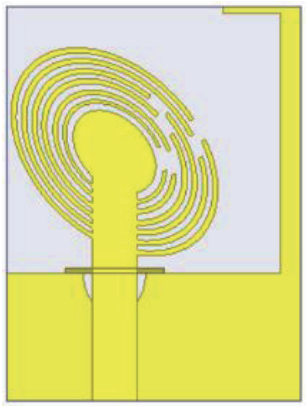

Figure 6. Loading of the strip.

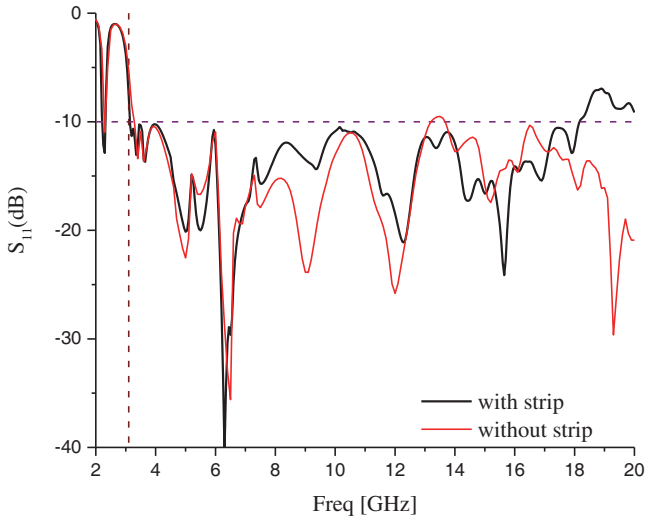

Figure 7. S_{11} coefficient of the final design.

resonance at around 2.5 GHz which is suitable also for 2.45 GHz ISM band applications.

The last step consists of loading the feed line with a crossing strip (Fig. 6). This shows an improvement in the impedance bandwidth (Fig. 7), where it can be noticed that the new bandwidth ranges from 3.1 to 18.1 GHz.

3. RESULTS AND DISCUSSIONS

To validate the proposed concept and HFSS simulated results, a prototype antenna is fabricated and measured. Fig. 8 shows photographs of the design fabricated according to the aforementioned parameters.

The surface current distributions describing the radiation operation for different operating frequencies are presented in Fig. 9. The relationship between the current path along the rings lengths and the resonance frequency is critical because it determines the antenna physical dimensions, which in turn determine the antenna's performance characteristics such as radiation pattern, gain, and impedance matching.

The proposed structure works in the frequency range 3.1–18.1 GHz realizing an impedance fractional bandwidth (FBW) of 141.51%. The L shaped strip in the ground plane shows a considerable effect at frequencies less than 6 GHz (Figs. 9(a)–9(h)). As the length of the current path in the antenna decreases, the operating frequency increases. This is because a shorter current path is required to achieve resonance

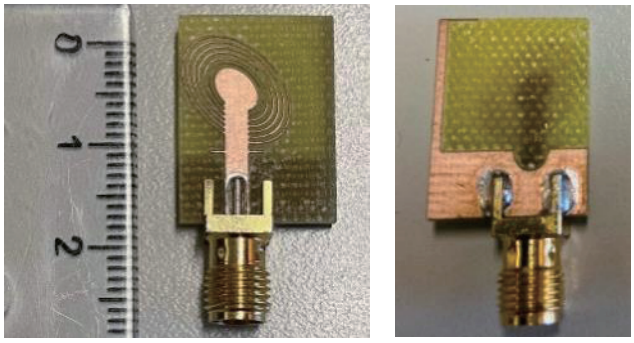

(a) (b)

Figure 8. Prototype of fabricated UWB antenna (a) top view and (b) bottom view.

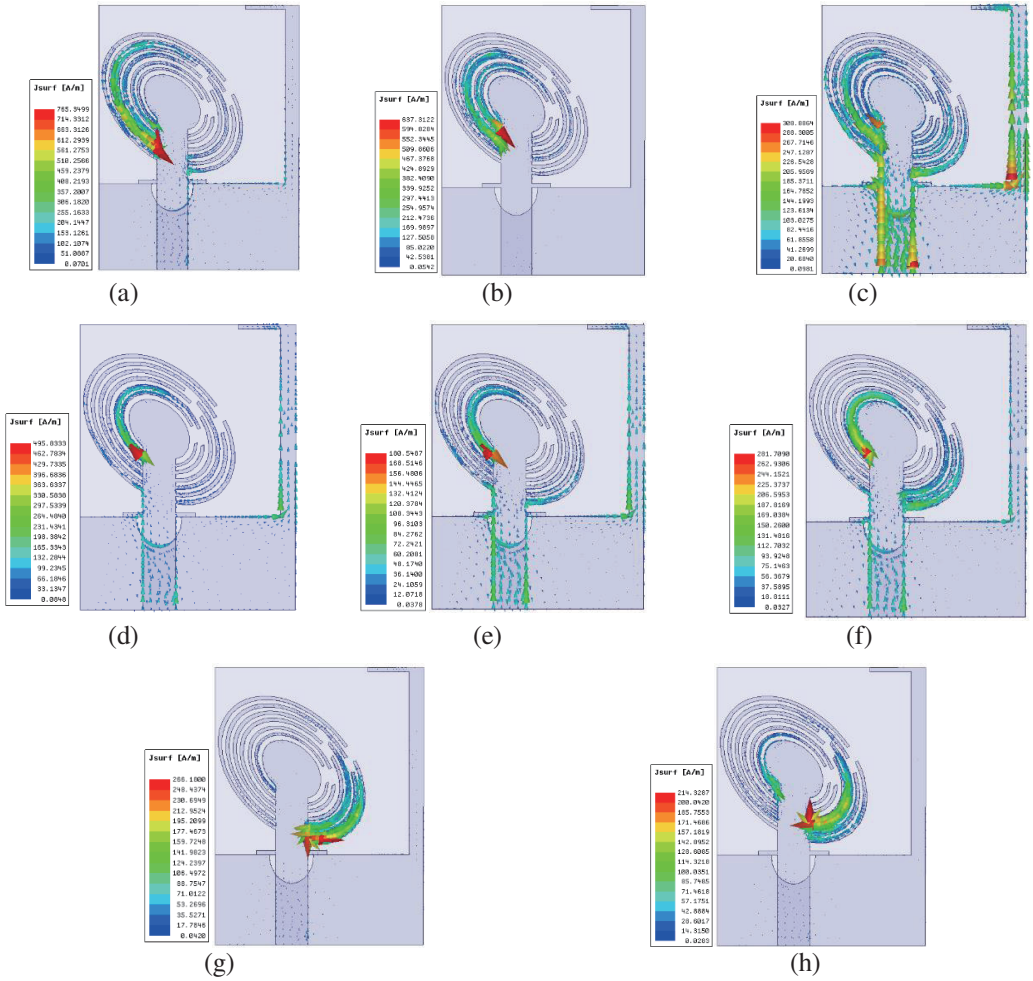

(a) (b) (c) (d) (e) (f) (g) (h)

Figure 9. Surface current distributions at (a) 3.1 GHz, (b) 3.5 GHz, (c) 3.7 GHz, (d) 3.8 GHz, (e) 4.2 GHz, (f) 4.5 GHz, (g) 5 GHz and (h) 6 GHz.

at higher frequencies. Conversely, at lower frequencies, a longer current path is required. The current path lengths along different rings are about quarter wavelengths at corresponding resonance frequencies. Therefore, the use of multiple rings created multiple resonance frequencies and widened the antenna bandwidth considerably.

Figure 10 shows the simulated and measured S-parameters of the proposed antenna. Though some differences in peak values can be noticed between simulations and measurements, which may be attributed to human errors introduced during the measurement process in the anechoic chamber, good agreement is observed, and both satisfy the bandwidth requirements ($< -10\,\text{dB}$).

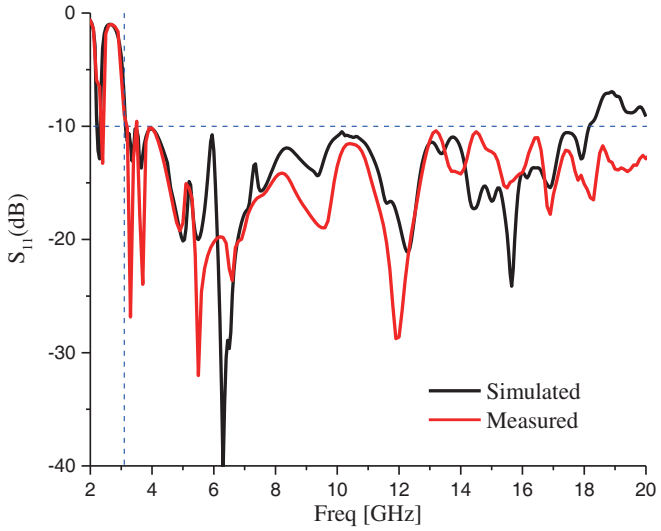

Figure 10. Simulated and measured S_{11} results of the final design.

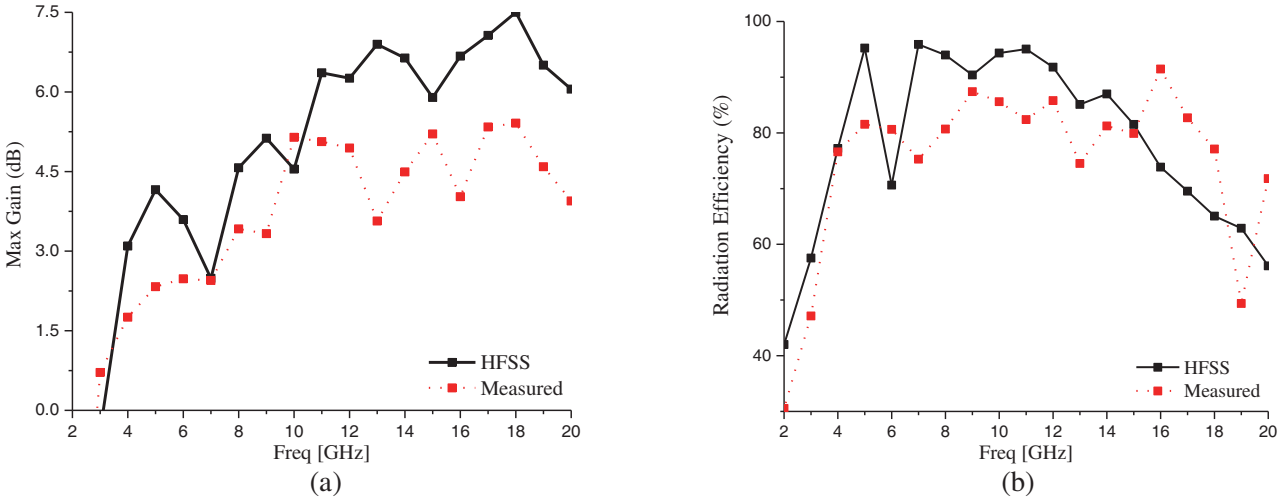

Figure 11. Simulated and measured antenna parameters, (a) total gain and (b) efficiency.

Figure 11 shows the gain and efficiency of the proposed UWB antenna. We notice that the measured gain varies between 0.75 and 5.4 dBi in the operating frequency band and tends to increase with frequency; this may be due to high order modes having higher values of gain proportional to frequency squared ($G \propto f^2$) [50, 51]. The efficiency fluctuates between 50% and 90% in the operating band and tends to decrease at higher frequencies. This can be explained by the fact that the efficiency is affected by losses in the conducting patch and the dielectric substrate which increase with frequency.

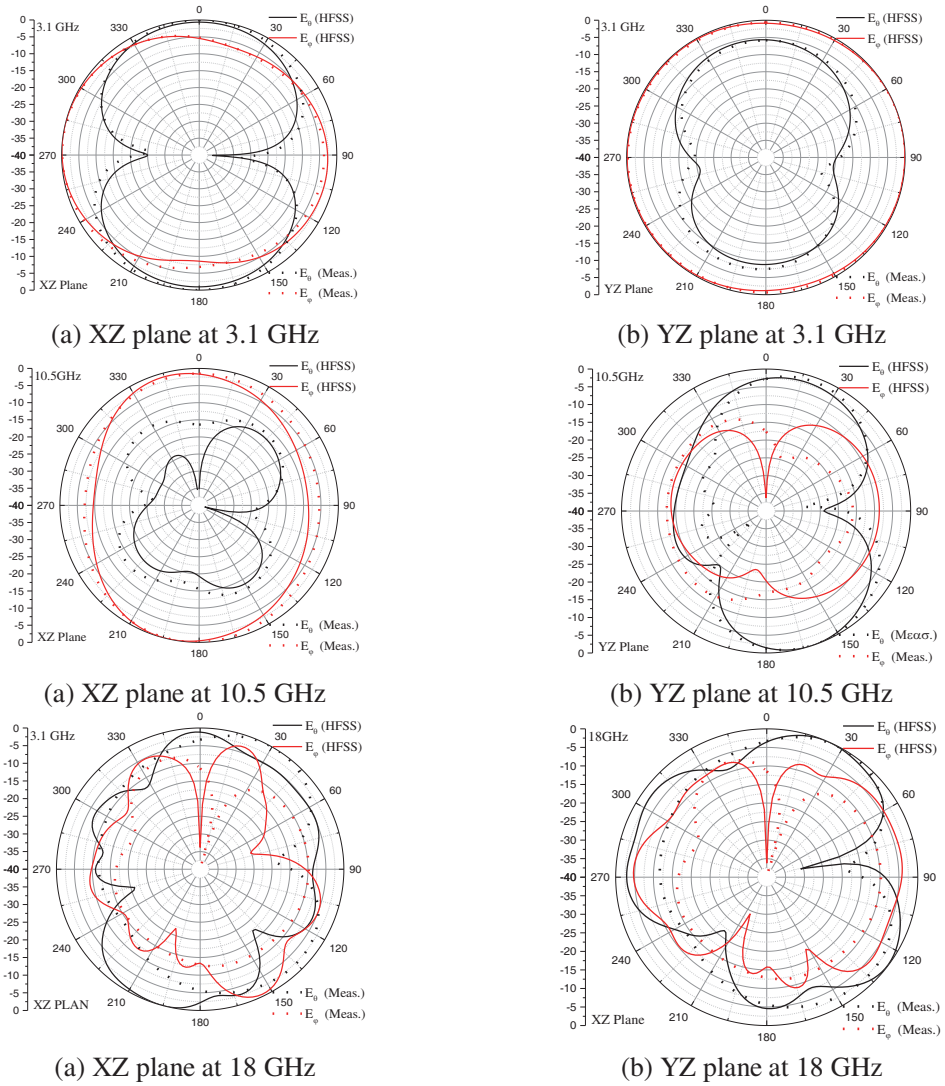

(a) XZ plane at 3.1 GHz (b) YZ plane at 3.1 GHz

(a) XZ plane at 10.5 GHz (b) YZ plane at 10.5 GHz

(a) XZ plane at 18 GHz (b) YZ plane at 18 GHz

Figure 12. Simulated and measured radiation patterns at different frequencies in XZ and YZ planes.

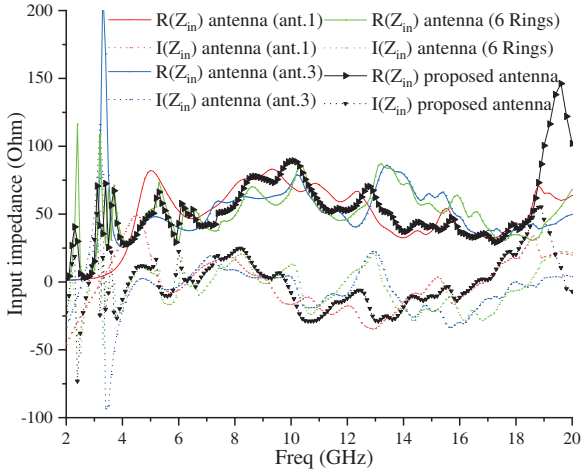

Figure 13. Input impedance of the design steps.

Some mismatch between simulations and experiments is observed due to experimental inaccuracies and simulation assumptions. However, this mismatch is bound and lies within admissible margins.

The simulated radiation patterns, in the XZ and YZ planes, for 3.1 GHz, 10.5 GHz, and 18 GHz compared with measurements, show a quasi-omnidirectional pattern in both planes (Fig. 12).

The rings shape allows the creation of 3 radiating modes with impedance of the order of 100, 75, and 72 Ohms, respectively. The loading of the stub allows these radiating modes to be well matched (Fig. 13).

Table 2 summarizes the results of a comparative study with previous works (all structures are planar monopoles). The proposed UWB monopole antenna shows clear advantages in terms of compactness, gain, and frequency bandwidth.

Table 2. Comparison with recently published UWB monopole antennas (λ_0 is the free space wavelength at the lower frequency).

Year	Ref	Bandwidth (GHz)	FBW (%)	Area (mm^2)	Max Gain (dBi)	Area (λ_0^2)
2020	[30]	3–11	114.29	24×30	4.5	0.24×0.3
2020	[7]	2.2–9.8	126.67	31×45	5.5	0.23×0.33
2020	[53]	2.19–13.95	145.72	26×27	5	0.19×0.2
2020	[54]	1.98–10.54	136.74	31.3×34.9	4	0.21×0.23
2020	[23]	3.42–11.79	110.06	24×28	4.08	0.27×0.32
2020	[56]	3.05–11.9	118.39	61×61	9.68	0.62×0.62
2021	[35]	3.19–15.32	131.06	18×26	4.5	0.19×0.28
2021	[52]	2.95–11.82	120.11	20×28	3.89	0.20×0.28
2021	[18]	2.5–10.6	123.66	38×48	8.4	0.32×0.40
2021	[20]	3.1–10.6	109.49	32×38	5.75	0.33×0.39
2021	[39]	2.4-10.5	125.58	20×26	7	0.16×0.21
2022	[19]	3.2–11.7	114.09	23×28	9.8	0.25×0.30
2022	[37]	3–12.7	123.57	24×30	3.6	0.24×0.30
2022	[38]	2.8–10.6	116.42	17×23	4.9	0.16×0.21
2022	[53]	3–11	114.29	22×25	4.1	0.22×0.25
2023	[57]	3.5–10.4	99.28	30×35	NR	0.35×0.41
2023	[58]	3.63–21.94	143.21	16×22	6.0	0.19×0.27
Proposed antenna		3.1–18.1	141.51	15×20	5.4	0.16×0.21

NR: not reported

4. CONCLUSION

A novel low-profile miniaturized UWB microstrip antenna is presented. The proposed antenna is designed and simulated using HFSS 15 and experimentally validated. The proposed design has been fabricated and tested as proof of concept. The proposed low-profile UWB antenna structure achieves a wide impedance bandwidth (141.51%), stable gain, and omnidirectional patterns using six concentric open rings.

The antenna shows convincing results that are suitable for UWB applications and advantages in comparison with other designs for the same applications in terms of overall size and some parameters such as high gain and high efficiency that achieved a peak of 5.4 dBi and 90%, respectively.

ACKNOWLEDGMENT

This work is supported by the Moore4Medical project, funded within ECSEL JU in collaboration with the EU H2020 Framework Programme (H2020/2014-2020) under grant agreement H2020-ECSEL-2019-IA-876190, and Fundação para a Ciência e Tecnologia (ECSEL/0006/2019). Funded also by the FCT/MEC through national funds and when applicable co-financed by the ERDF, under the PT2020 Partnership Agreement under the UID/EEA/50008/2020 project. This work is supported in part by the DGRSDT (Ministry of Higher Education and Scientific Research), Algeria.

REFERENCES

1. Balanis, C. A., *Antenna Theory: Analysis and Design*, 4th Edition, John Wiley & Sons, ISBN: 978-1-118-642060-1, Hoboken, New Jersey, USA, 2016.
2. Sun, C., "A design of compact ultrawideband circularly polarized microstrip patch antenna," *IEEE Transactions on Antennas and Propagation*, Vol. 67, No. 9, 6170–6175, 2019, DOI: 10.1109/TAP.2019.2922759.
3. Kumar, O. P., P. Kumar, T. Ali, et al., "Ultrawideband antennas: Growth and evolution," *Micromachines*, Vol. 13, 60, 2022, DOI: 10.3390/mi13010060.
4. Li, W., D. Li, G. Dong, et al., "High-stability organic red-light photodetector for narrowband applications," *Laser & Photonics Reviews*, Vol. 10, No. 3, 473–480, 2016, DOI: 10.1002/lpor.201500279.
5. Li, W. H. and G. Zheng, "Photoactivatable fluorophores and techniques for biological imaging applications," *Photochemical & Photobiological Sciences*, Vol. 11, No. 3, 460–471, 2012, DOI: 10.1039/C2PP05342J.
6. Coppens, D., A. Shahid, S. Lemey, et al., "An overview of UWB standards and organizations (IEEE 802.15.4, FiRa, Apple): Interoperability aspects and future research directions," *IEEE Access*, Vol. 10, 70219–70241, 2022, DOI: 10.1109/ACCESS.2022.3187410.
7. Serria, E. A. and M. I. Hussein,, "Implications of metamaterial on ultra-wide band microstrip antenna performance," *Crystals*, Vol. 10, No. 8, 677, 2020, DOI: 10.3390/cryst10080677.
8. Saxena, S., B. K. Kanaujia, S. Dwari, et al., "A compact dual-polarized MIMO antenna with distinct diversity performance for UWB applications," *IEEE Antennas and Wireless Propagation Letters*, Vol. 16, 3096–3099, 2017, DOI: 10.1109/LAWP.2017.2762426.
9. Parthiban, N. and M. M. Ismail, "Design and analysis of quad-band notch characteristics UWB antenna using SLR circuits," *Progress In Electromagnetics Research C*, Vol. 124, 11–22, 2022, DOI:10.2528/PIERC22060901.
10. Ahajjam, Y., O. Aghzout, J. M. Catala-Civera, F. Peñaranda-Foix, and A. Driouach, "Range distance measurements using an UWB tapered slot 0.43 GHz to 6 GHz antenna for IoT application," *Procedia Manufacturing*, Vol. 32, 710–716, 2019, DOI: 10.1016/j.promfg.2019.02.277.
11. Chehri, A. and H. T. Mouftah, "Internet of things-integrated IR-UWB technology for healthcare applications," *Concurrency and Computation: Practice and Experience*, Vol. 32, No. 2, e5454, 2020, DOI: 10.1002/cpe.5454.
12. Abushakra, F., N. Jeong, D. N. Elluru, et al., "A miniaturized ultra-wideband radar for UAV remote sensing applications," *IEEE Microwave and Wireless Components Letters*, Vol. 32, No. 3, 198–201, March 2022, DOI: 10.1109/LMWC.2021.3129153.
13. Jayant, S., G. Srivastava, and S. Kumar, "Quad-port UWB MIMO footwear antenna for wearable applications," *IEEE Transactions on Antennas and Propagation*, Vol. 70, No. 9, 7905–7913, September 2022, DOI: 10.1109/TAP.2022.3177481.
14. Fiser, O., V. Hruby, J. Vrba, et al., "UWB bowtie antenna for medical microwave imaging applications," *IEEE Transactions on Antennas and Propagation*, Vol. 70, No. 7, 5357–5372, July 2022, DOI: 10.1109/TAP.2022.3161355.
15. Rafique, U., S. Pisa, R. Cicchetti, et al., "Ultra-wideband antennas for biomedical imaging applications: A survey," *Sensors*, Vol. 22 No. 9, 2022, DOI: 10.3390/s22093230.

16. Lin, X., Y. Chen, Z. Gong, et al., "Ultrawideband textile antenna for wearable microwave medical imaging applications," *IEEE Transactions on Antennas and Propagation*, Vol. 68, No. 6, 4238–4249, 2020, DOI: 10.1109/TAP.2020.2970072.
17. Tan, W., X. Shan, and Z. Shen, "Ultrawideband circularly polarized antenna with shared semicircular patches," *IEEE Transactions on Antennas and Propagation*, Vol. 69, No. 6, 3555–3559, 2020, DOI: 10.1109/TAP.2020.3037754.
18. Gopi, D., A. R. Vadaboyina, and J. R. K. Dabbakuti, "DGS based monopole circular-shaped patch antenna for UWB applications," *SN Applied Sciences*, Vol. 3, No. 2, 1–12, 2021, DOI: 10.1007/s42452-020-04123-w.
19. Kumar, O. P., P. Kumar, and T. Ali, "A compact dual-band notched UWB antenna for wireless applications," *Micromachines*, Vol. 13, No. 12, 2022, DOI: 10.3390/mi13010012,
20. Sura, P. R. and K. A. Kumar, "Design of dual-band notched UWB antenna loaded with split ring resonators for wide band rejection," *International Journal of Electronics Letters*, 1–13, 2022, DOI: 10.1080/21681724.2021.2025437.
21. Jeong, M., N. Hussain, A. Abbas, et al., "Performance improvement of microstrip patch antenna using a novel double-layer concentric rings metaplate for 5G millimeter wave applications," *International Journal of RF and Microwave Computer-Aided Engineering*, Vol. 31, No. 2, e22509, 2021, DOI: 10.1002/mmce.22509.
22. Kaur, N., J. S. Sivia, and M. Kumar, "Design of nested circular ring-shaped ultra-wideband antenna loaded with SRR and defected ground plane," *Wireless Pers Commun.*, Vol. 123, 2985–3001, 2022, DOI: 10.1007/s11277-021-09272-8.
23. Devana, V. K. R. and A. M. Rao, "Design and analysis of dual band-notched UWB antenna using a slot in feed and asymmetrical parasitic stub," *IETE Journal of Research*, 1–11, September 2020, DOI: 10.1080/03772063.2020.1816226.
24. Alani, S., Z. Zakaria, T. Saeidi, A. Ahmad, et al., "Microwave imaging of breast skin utilizing elliptical UWB antenna and reverse problems algorithm," *Micromachines*, Vol. 12, No. 647, 2021, DOI:10.3390/mi12060647.
25. Nguyen, D. H., V. Krozer, J. Moll, and G. Zimmer, "Ultra-wideband on-body elliptical monopole antenna," *Electronics Letters*, Vol. 57, No. 5, 200–202, 2021, DOI: 10.1049/ell2.12085.
26. Khajevandi, A. and H. Oraizi, "Design of a circularly polarized microstrip slot antenna using Minkowski fractal by the characteristic mode theory," *Electronics Letters*, Vol. 58, No. 9, 352–355, 2022, DOI: 10.1049/ell2.12466.
27. Rao, N., "Gain enhancement of miniaturized fractal antenna with help of complementary fractal lens," *Wireless Pers Commun.*, Vol. 123, 229–240, 2022, DOI: 10.1007/s11277-021-09128-1.
28. Rahim, A. and P. K. Malik, "Analysis and design of fractal antenna for efficient communication network in vehicular model," *Sustainable Computing: Informatics and Systems*, Vol. 31, 100586, 2021, DOI: 10.1016/j.suscom.2021.100586.
29. Sufian, M. A., N. Hussain, A. Abbas, et al., "Mutual coupling reduction of a circularly polarized MIMO antenna using parasitic elements and DGS for V2X communications," *IEEE Access*, Vol. 10, 56388–56400, 2022, DOI: 10.1109/ACCESS.2022.3177886.
30. Du, Y., X. Wu, J. Sidén, and G. Wang, "Design of ultra-wideband antenna with high-selectivity band notches using fragment-type etch pattern," *Microwave and Optical Technology Letters*, Vol. 62, No. 2, 912–918, 2020, DOI: 10.1002/mop.32103.
31. Baudha, S. and M. V. Yadav, "A compact ultra-wide band planar antenna with corrugated ladder ground plane for multiple applications," *Microwave and Optical Technology Letters*, Vol. 61, No. 5, 1341–1348, 2019, DOI: 10.1002/mop.31710.
32. Hotta, S., S. Baudha, B. B. Mangaraj, et al., "A compact, ultrawide band planar antenna with modified circular patch and a defective ground plane for multiple applications," *Microwave and Optical Technology Letters*, Vol. 61, No. 9, 2088–2097, 2019, DOI: 10.1002/mop.31867.
33. Padhi, J., A. Kumar, and G. S. Reddy, "Parasitic element loaded efficient electrically small antenna for indoor wireless applications," *Microwave and Optical Technology Letters*, Vol. 64, No. 10, 1793–1799, 2022, DOI: 10.1002/mop.33365.

34. Tran, H. H. and N. Nguyen-Trong, "Performance enhancement of MIMO patch antenna using parasitic elements," *IEEE Access*, Vol. 9, 30011–30016, 2021, DOI: 10.1109/ACCESS.2021.3058340.
35. Addepalli, T., A. Desai, I. Elfergani, et al., "8-port semi-circular Arc MIMO antenna with an inverted L-strip loaded connected ground for UWB applications," *Electronics*, Vol. 10, No. 12, 1476, 2021, DOI: 10.3390/electronics10121476.
36. Deshmukh, V. and S. Chorage, "Frequency reconfigurable patch antenna using slot, slits and defected ground structures: parametric analysis," *Australian Journal of Electrical and Electronics Engineering*, Vol. 19, No. 2, 171–184, 2022, DOI: 10.1080/1448837X.2021.2023077.
37. Khan, M., A. Rafique, U. Savci, et al., "Ultra-wideband pentagonal fractal antenna with stable radiation characteristics for microwave imaging applications," *Electronics*, Vol. 11, No. 2061, 2022, DOI: 10.3390/ELECTRONICS11132061.
38. Zaidi, A., W. A. Awan, A. Ghaffar, M. S. Alzaidi, M. Alsharef, D. H. Elkamchouchi, and T. E. Alharbi, "A low profile ultra-wideband antenna with reconfigurable notch band characteristics for smart electronic systems," *Micromachines*, Vol. 13, No. 11, 1803, 2022, DOI: 10.3390/MI13111803.
39. Garg, R. K., M. V. D. Nair, S. Singhal, and R. Tomar, "A miniaturized ultra-wideband antenna using "modified" rectangular patch with rejection in WiMAX and WLAN bands," *Microwave and Optical Technology Letters*, Vol. 63, No. 4, 1271–1277, 2021, DOI: 10.1002/MOP.32732.
40. Yang, H. C., X. Y. Liu, Y. Fan, et al., "Flexible circularly polarized antenna with axial ratio bandwidth enhancement for off-body communications," *IET Microwaves, Antennas & Propagation*, Vol. 15, No. 7, 754–767, 2021, DOI: 10.1049/mia2.12081.
41. Awan, W. A., M. Husain, M. Alibakhshikenari, et al., "Band enhancement of a compact flexible antenna for WLAN, Wi-Fi and C-band applications," *Proceedings of the International Symposium on Antennas and Propagation (ISAP)*, 1–2, Taipei, Taiwan, 2021, DOI: 10.23919/ISAP47258.2021.9614454.
42. Mondal, K., "Axial Ratio (AR) and impedance bandwidth (IBW) enhancement of circular polarized (CP) monopole antenna," *AEU — International Journal of Electronics and Communications*, Vol. 134, 153649, 2021, DOI: 10.1016/j.aeue.2021.153649.
43. Elwi, T. A., D. A. Jassim, and H. H. Mohammed, "Novel miniaturized folded UWB microstrip antenna-based metamaterial for RF energy harvesting," *International Journal of Communication Systems*, Vol. 33, No. 6, e4305, 2020, DOI: 10.1002/dac.4305.
44. Soerbakti, Y., R. F. Syahputra, M. D. H. Gamal, D. Irawan, E. H. Putra, and R. S. Darwis, "Improvement of low-profile microstrip antenna performance by hexagonal-shaped SRR structure with DNG metamaterial characteristic as UWB application," *Alexandria Engineering Journal*, Vol. 61, No. 6, 4241–4252, 2022, DOI: 10.1016/j.aej.2021.09.048.
45. Wang, L. and S. Kumar, "Compact ultra-wideband antenna for microwave imaging applications," *Computational and Experimental Simulations in Engineering, ICCES 2022, Mechanisms and Machine Science*, H. Dai, Editor, Vol. 119, Springer, Cham, 2023, DOI: 10.1007/978-3-031-02097-1_16.
46. Li, H., H. Zhang, Y. Kong, and C. Zhou, "Flexible dual-polarized UWB antenna sensors for breast tumor detection," *IEEE Sensors Journal*, Vol. 22, No. 13, 13648–13658, 2022, DOI: 10.1109/JSEN.2022.3180356.
47. Alsath, M. G. N. and M. Kanagasabai, "Compact UWB monopole antenna for automotive communications," *IEEE Trans. Antennas Propag.*, Vol. 63, 4204–4208, 2015, DOI: 10.1109/TAP.2015.2447006.
48. Rohan, C., J. Audet, and A. Keating, "Small split-ring resonators as efficient antennas for remote lora IoT systems — A path to reduce physical interference," *Sensors*, Vol. 21, No. 23, 7779, 2021, DOI: 10.3390/s21237779.
49. Garg, R., *Microstrip Antenna Design Handbook*, Artech House, Boston, 2000.
50. Balanis, C. A., "Antenna theory: A review," *Proceedings of the IEEE*, Vol. 80, No. 1, 7–23, 1992.

51. Gangwar, R. K., A. Sharma, M. Gupta, and S. Chaudhary, "Hybrid cylindrical dielectric resonator antenna with HE 11δ and HE 12δ mode excitation for wireless applications," *International Journal of RF and Microwave Computer-Aided Engineering*, Vol. 26, No. 9, 812–818, 2016.
52. Singh, G. and U. Singh, "Multi-objective naked mole-rat algorithm for UWB antenna design," *IETE Journal of Research*, 2021, DOI:10.1080/03772063.2021.1912657.
53. Garg, R. K., M. V. D. Nair, S. Singhal, and R. Tomar, "A new type of compact ultra-wideband planar fractal antenna with WLAN band rejection," *Microwave and Optical Technology Letters*, Vol. 62, No. 7, 2537–2545, 2020, DOI: 10.1002/mop.32304.
54. Shome, P. P., T. Khan, and R. H. Laskar, "CSRR-loaded UWB monopole antenna with electronically tunable triple band-notch characteristics for cognitive radio applications," *Microw Opt Technol Lett.*, Vol. 62, 2919–2929, 2020, DOI: 10.1002/mop.32394.
55. Ahmad, S., U. Ijaz, S. Naseer, A. Ghaffar, M. A. Qasim, F. Abrar, and R. Abd-Alhameed, "A jug-shaped CPW-fed ultra-wideband printed monopole antenna for wireless communications networks," *Applied Sciences*, Vol. 12, No. 2, 821, 2022, DOI: 10.3390/app12020821.
56. Al-Gburi, A. J. A., I. B. M. Ibrahim, M. Y. Zeain, and Z. Zakaria, "Compact size and high gain of CPW-fed UWB strawberry artistic shaped printed monopole antennas using FSS single layer reflector," *IEEE Access*, Vol. 8, 92697–92707, 2020.
57. Vinoth, J. C., S. Ramesh, Z. Z. Abidin, S. A. Qureshi, S. Chitra, E. Saranya, and G. Sneha, "Planar edged UWB antenna for water quality measurement," *Progress In Electromagnetics Research C*, Vol. 130, 83–93, 2023.
58. Ponnapalli, V. L. N. P., S. Karthikeyan, J. L. Narayana, and V. N. K. R. Devana, "A compact novel lamp slotted WLAN band notched UWB antenna integrated with Ku band," *Progress In Electromagnetics Research C*, Vol. 129, 89–98, 2023.